Inflammatory stimuli induce acyl-CoA thioesterase 7 and remodeling of phospholipids containing unsaturated long (⩾C20)-acyl chains in macrophages[S]

Valerie Z. Wall,*,† Shelley Barnhart,* Farah Kramer,* Jenny E. Kanter,* Anuradha Vivekanandan-Giri,§ Subramaniam Pennathur,§ Chiara Bolego, Jessica M. Ellis,§§,*** Miguel A. Gijón,††† Michael J. Wolfgang,*** and Karin E. Bornfeldt[1],*,†**

Department of Medicine,* Division of Metabolism, Endocrinology and Nutrition, and Department of Pathology,† UW Medicine Diabetes Institute, University of Washington, Seattle, WA; Department of Internal Medicine,§ University of Michigan, Ann Arbor, MI; Department of Pharmaceutical and Pharmacological Sciences,** University of Padova, Padova, Italy; Department of Nutrition Science,§§ Purdue University, West Lafayette, IN; Department of Biological Chemistry,*** Johns Hopkins University School of Medicine, Baltimore, MD; and Department of Pharmacology,††† University of Colorado Denver, Aurora, CO

Abstract Acyl-CoA thioesterase 7 (ACOT7) is an intracellular enzyme that converts acyl-CoAs to FFAs. ACOT7 is induced by lipopolysaccharide (LPS); thus, we investigated downstream effects of LPS-induced induction of ACOT7 and its role in inflammatory settings in myeloid cells. Enzymatic thioesterase activity assays in WT and ACOT7-deficient macrophage lysates indicated that endogenous ACOT7 contributes a significant fraction of total acyl-CoA thioesterase activity toward C20:4-, C20:5-, and C22:6-CoA, but contributes little activity toward shorter acyl-CoA species. Lipidomic analyses revealed that LPS causes a dramatic increase, primarily in bis(monoacylglycero)phosphate species containing long (⩾C20) polyunsaturated acyl-chains in macrophages, and that the limited effect observed by ACOT7 deficiency is restricted to glycerophospholipids containing 20-carbon unsaturated acyl-chains. Furthermore, ACOT7 deficiency did not detectably alter the ability of LPS to induce cytokines or prostaglandin E_2 production in macrophages. Consistently, although ACOT7 was induced in macrophages from diabetic mice, hematopoietic ACOT7 deficiency did not alter the stimulatory effect of diabetes on systemic inflammation or atherosclerosis in LDL receptor-deficient mice. Thus, inflammatory stimuli induce ACOT7 and remodeling of phospholipids containing unsaturated long (⩾C20)-acyl chains in macrophages, and, although ACOT7 has preferential thioesterase activity toward these lipid species, loss of ACOT7 has no major detrimental effect on macrophage inflammatory phenotypes.—Wall, V. Z., S. Barnhart, F. Kramer, J. E. Kanter, A. Vivekanandan-Giri, S. Pennathur, C. Bolego, J. M. Ellis, M. A. Gijón, M. J. Wolfgang, and K. E. Bornfeldt. **Inflammatory stimuli induce acyl-CoA thioesterase 7 and remodeling of phospholipids containing unsaturated long (⩾C20)-acyl chains in macrophages. *J. Lipid Res.* 2017.** 58: **1174–1185.**

Supplementary key words atherosclerosis • cytokines • diabetes • fatty acid • inflammation • lipidomics

Monocytes and macrophages are an essential component of the innate immune response. When activated by pathogens, macrophages secrete cytokines, contributing to immune cell recruitment and activation. Once the pathogen is cleared, this inflammatory response is resolved. Dysregulation of the inflammatory response, however, underlies several disease processes. It is becoming increasingly clear that intracellular FA handling plays an important role in modulating the inflammatory response (1–6). Previous studies have revealed that macrophages deficient in the FA binding protein FABP4 (aP2) exhibit reduced inflammatory activation, reduced activation of NF-κB, and

This work was supported by National Heart, Lung, and Blood Institute Grants R01HL062887, R01HL126028, and P01HL092969; National Institute of Diabetes and Digestive and Kidney Diseases Grant DP3DK108209 (K.E.B.); National Institutes of Health Grants DK082841 and DK 081943 (S.P.); and National Institute of Neurological Disorders and Stroke Grant NS072241 (M.J.W.). Part of the study was supported by the Diabetes Research Center, University of Washington Grant P30 DK017047. Acyl-CoAs were analyzed through the Molecular Phenotyping Core, Michigan Nutrition and Obesity Center Grant P30 DK089503. J.E.K. was in part supported by the McAbee Fellowship in Diabetes Research. V.Z.W. was supported by the Samuel and Althea Stroum Fellowship in Diabetes Research and Cell and Molecular Biology Training Grant T32HL007828. The content is solely the responsibility of the authors and does not necessarily represent the official views of the National Institutes of Health.

Manuscript received 27 March 2017.

Published, JLR Papers in Press, April 17, 2017
DOI https://doi.org/10.1194/jlr.M076489

Abbreviations: ACOT, acyl-CoA thioesterase; ACSL, acyl-CoA synthetase; BMDM, bone marrow-derived macrophage; BMP, bis(monoacylglycero)phosphate; LPS, lipopolysaccharide; PG, prostaglandin; STZ, streptozotocin; TLR4, Toll-like receptor 4.

[1]To whom correspondence should be addressed.
e-mail: bornf@uw.edu

[S] The online version of this article (available at http://www.jlr.org) contains a supplement.

a concomitant increase in PPAR-γ activation (1). The anti-inflammatory effects associated with loss of FABP4 in macrophages have subsequently been shown to be due to increased expression of uncoupling protein 2 (4) and sirtuin 3 (6), likely because of increased levels of free intracellular MUFAs. Consistently, inhibition of FABP4 prevents atherosclerosis in mice (2). Similar results have been found by KO of FABP5 (3). Furthermore, long-chain acyl-CoA synthetase 1 (ACSL1), an enzyme that converts FFAs into their acyl-CoA derivatives, is induced by Toll-like receptor 4 (TLR4) activation in macrophages, and its deletion in myeloid cells results in protection against early atherosclerosis in diabetic mice (5). More recently, elegant studies have demonstrated that unsaturated FAs (including omega-6 and -3 FAs) are increased in the late phase (12–24 h) of TLR4 activation in macrophages, concomitant with induction of enzymes involved in MUFA and PUFA metabolism, and that SREBP1 regulates this late resolution phase of the inflammatory response (6).

We therefore investigated the role of unsaturated FA handling in regulation of inflammation and atherosclerosis by studying one of the acyl-CoA thioesterases (ACOTs) induced by TLR4 activation by lipopolysaccharide (LPS) in macrophages, ACOT7. ACOTs hydrolyze the thioester bond on acyl-CoAs, but their cellular functions have just recently begun to be elucidated. There are 15 known ACOTs in mice, each with differential tissue and intracellular localization, transcriptional regulation, and acyl-CoA substrate preference (7–10). Only a few studies to date have investigated the function of ACOTs in vivo (11–18). These studies have revealed that ACOTs are important mediators of FA and acyl-CoA channeling into specific fates, and that the processes mediated by ACOTs appear to require rapid and dynamic interconversion between FFAs and acyl-CoAs. Thus, ACOT2 promotes hepatic FA oxidation, which requires acyl-CoA formation (13). ACOT13 deficiency protects against hepatic triglyceride accumulation in fat-fed mice and increases energy expenditure after cold exposure (14, 15), and likewise, ACOT11 deficiency protects against obesity by increasing energy expenditure (16, 18). ACOT15 is involved in cardiolipin remodeling (11).

ACOT7 is highly expressed in neurons (19, 20), and a neuron-specific ACOT7-deficient mouse exhibits elevated levels of lysophospholipid and sphingosine in the brain (12). ACOT7 has been shown to have preferential activity toward arachidonoyl-CoA (20:4-CoA) over saturated acyl-CoAs in macrophages (21), but also to act on other long-chain acyl-CoAs (21, 22). Forced expression of an active ACOT7 mutant has been found to suppress prostaglandin D_2 (PGD_2) and PGE_2 production under basal conditions in a macrophage cell line (21). Overexpression of ACOT7 in pancreatic β cells lowered acyl-CoA levels, consistent with what one would predict based on the enzymatic activity of ACOT7 (17). On the contrary, ACOT7 deficiency results in markedly increased levels of free unsaturated FAs in neurons (12), suggesting that compensation may exist for loss of ACOT7 in some cell types.

We investigated the role of ACOT7 in two models of inflammation in which altered FA handling in macrophages is thought to contribute to the inflammatory phenotype: LPS stimulation of macrophages in vitro and an in vivo mouse model of diabetes. Our results demonstrate that ACOT7 is induced by TLR4 through its adaptor protein MyD88 and by diabetes in macrophages and that classical $Ly6C^{high}$ monocytes exhibit elevated ACOT7 gene expression, as compared with $Ly6C^{low}$ monocytes. We demonstrate that LPS causes a marked shift in acyl-chain composition of bis(monoacylglycero)phosphate (BMP), a phospholipid present in late endosomes and lysosomes (23), from shorter saturated and monounsaturated BMPs to BMPs containing long-chain (C20 and C22) unsaturated acyl-chains in the resolution phase of the inflammatory response. Furthermore, ACOT7 contributes a significant fraction of total ACOT activity toward arachidonoyl-CoA (C20:4-CoA), docosahexaenoyl-CoA (C22:6-CoA), and eicosapentaenoyl-CoA (C20:5-CoA) in macrophages, and the limited effect of ACOT7 deficiency on glycerophospholipids is restricted to species containing 20-carbon unsaturated acyl-chains. However, loss of ACOT7 is not sufficient to counter the striking effect of LPS on BMP acyl-chain composition or to alter the inflammatory response in macrophages.

MATERIALS AND METHODS

Mice

All mice were on the C57BL/6 background. $Acot7^{-/-}$ mice were generated by crossing $Acot7^{fl/fl}$ mice (12) to mice expressing Cre recombinase from the germline (Jax 006054) (24). Mice carrying a deleted allele of *Acot7* were then bred to homozygosity in the absence of Cre recombinase. For additional lipidomics, $Acot7^{fl/fl}$ mice were crossed with $Lys2^{Cre/Cre}$ mice to generate bone marrow-derived macrophages (BMDMs) lacking ACOT7 with $Acot7^{WT/WT}$; $Lys2^{Cre/Cre}$ littermates used as controls. Female LDL receptor-deficient ($Ldlr^{-/-}$) mice for atherosclerosis studies were obtained from Jackson Labs (Bar Harbor, ME). Bones from $Tlr4^{-/-}$ mice were a generous gift from Dr. Linda Curtiss, the Scripps Research Institute, and bones from $Myd88^{-/-}$ mice and TRIF-deficient ($Ticam1^{-/-}$) mice were generously provided by Dr. Alan Aderem, Seattle Biomedical Research Institute, and Dr. Kelly D. Smith, University of Washington, Seattle. Bones from WT littermates were used as controls. All studies were approved by the Animal Care and Use Committee of the University of Washington. Mice were housed (maximum five per cage) in a specific pathogen-free barrier facility with a 12 h light/dark cycle with free access to food and water.

Sorting and RNA isolation of mouse blood monocyte and neutrophil populations

Retroorbital blood was harvested and purified of erythrocytes. Fluorescently labeled antibodies were added after addition of viability dye (diluted 1:10; eBioscience, San Diego, CA, catalog no. 65-0863) and an F_c blocking step (eBioscience, catalog no. 14-0161). The antibodies used included: APC-labeled:anti-CD115 (undiluted; eBioscience, clone AFS98), PECy7-labeled:anti-GR1 (diluted 1:20; eBioscience, clone RB6-8C5), and FITC-labeled:anti-CD45 (diluted 1:10; eBioscience, clone 30-F11). Cells were kept at 4°C during all steps in the staining protocol to minimize changes in mRNA. Cells were sorted on a FACS Aria 2 cell sorter directly into lysis buffer

(RNeasy Micro Kit, Qiagen, Valencia, CA). Cells were gated by forward and side scatter to remove debris, doublets were removed by FSC-H vs. FSC-W, and then cells were gated on viability dye to remove dead cells. Ly6C^{high} monocytes were considered CD45+/CD115+/GR1^{high}, Ly6C^{low} monocytes were CD45+/CD115+/GR1^{low}, and neutrophils were CD45+/CD115-/GR1^{high}. All flow cytometry included appropriate fluorescence minus one (FMO) controls. After cell sorting, mRNA from monocytes and neutrophils was extracted (RNeasy Micro Kit, Qiagen), and cDNA was made (SuperScript VILO, Thermo Scientific, Waltham, MA) according to manufacturers' instructions. Real-time quantitative PCR for gene expression was performed as described below.

Isolation and maintenance of BMDMs

BMDMs were harvested from freshly obtained bones or from bones shipped overnight on wet ice by syringe flushing with DMEM supplemented with 1% fungizone and 1% penicillin/streptomycin. Cells were purified of erythrocytes and maintained in DMEM (450 mg/dl glucose) containing 1% fungizone, 1% penicillin/streptomycin, 7% FBS, and 30% L-cell conditioned medium, as a source of macrophage colony-stimulating factor. For measurements of inflammatory responses, cells were stimulated with ultrapure LPS (*Escherichia. coli* 0111:B4, 10 or 0.1 ng/ml; List Biological Laboratories, Campbell, CA). Alternative activation was achieved by 24 h treatment with IL-4 (10 ng/ml; eBioscience; catalog no. 14-8041).

Generation of a retroviral vector for ACOT7 overexpression

Murine *Acot7* cDNA (Origene, Rockville, MD) was cloned into the retroviral pBM-IRES-PURO (pBM) vector. Phoenix ecotropic cells (Allele Biotechnology, San Diego, CA) were transfected with the empty pBM vector or pBM-ACOT7 vector by $CaCl_2$ transfection, according to Allele Biotechnology's instructions. Phoenix cells transfected with a pBM-enhanced green fluorescent protein vector were used to generate additional controls for some experiments. The day after transfection, the cells were passaged into medium containing 2 μg/ml puromycin for positive selection and then maintained in medium containing puromycin until virus collection when the cultures were ∼90% confluent. J774 macrophages or freshly harvested bone marrow cells were treated with DMEM (450 mg/dl glucose) containing 0.45 μM syringe-filtered retroviral medium, as well as HEPES (60 mmol/l), polybrene (4 μg/ml), 1% fungizone, 1% penicillin/streptomycin, and, in the case of BMDMs, 30% L-cell conditioned medium to induce macrophage differentiation. Retroviral medium was replaced after 48 h with DMEM (450 mg/dl glucose) containing 1% fungizone, 1% penicillin/streptomycin, and 10% FBS for J774 macrophages or with DMEM (450 mg/dl glucose) containing 1% fungizone, 1% penicillin/streptomycin, 7% FBS, and 30% L-cell conditioned medium for BMDMs. BMDMs were allowed to differentiate for 7–10 days before experiments. For measurements of inflammatory responses, cells were stimulated with LPS (5–10 ng/ml; *E. coli* 0111:B4; List Biological Laboratories) and, for BMDMs, IFN-γ (12 ng/ml; eBioscience, catalog no. 14-8311-63) for 18–24 h. In a subset of experiments, cells were treated with inhibitors of eicosanoid production: the cyclooxygenase 2 inhibitor CAY 10404 (500 nM; Cayman, Ann Arbor, MI) or the 5-lipoxygenase inhibitor CJ-13,610 (1–2 μM; Sigma-Aldrich, St. Louis, MO).

Knockdown of ACOT7 in thioglycollate elicited macrophages

For in vitro ACOT7 knockdown experiments, macrophages were harvested from the peritoneal cavity of C57BL/6 mice 5 days after injection of thioglycollate (5). Before plating the macrophages, *Acot7* siRNA (Life Technologies, Carlsbad, CA; catalog no. 4390771; i.d. s88465 and s211904) or negative control #2 siRNA (Life Technologies; catalog no. 4390846) was introduced by electroporation (Amaxa mouse macrophage nucleofector kit; Lonza, Cologne, Germany). The samples were electroporated in the Amaxa Nucleofector I device by using program Y-01, as described previously (25). A total of 3×10^6 cells/cuvette were electroporated and immediately plated in medium supplemented with 10% FBS, and medium and floating cells were removed 1 h later for adherence purification of macrophages. All experiments were performed by using RPMI 1640 medium (11.2 mM glucose) supplemented with 1% penicillin/streptomycin. For measurements of inflammatory responses, cells were stimulated with ultrapure LPS (*E. coli* 0111:B4, 10 ng/ml; List Biological Laboratories) for 48 h after electroporation, as ∼90% knockdown of ACOT7 protein was achieved at this time point.

Real-time PCR, ELISAs, and Western blots

Inflammatory mediators were quantified by real-time PCR and ELISAs. RNA isolation and the real-time PCR protocol were performed as described (5). Briefly, RNA was isolated by using RNeasy (Qiagen) or Nucleospin (Macherey-Nagel, Bethlehem, PA) RNA kits according to manufacturers' protocols and treated with DNase1 (1 μg/sample, Thermo Scientific) to remove trace DNA. Real-time PCR was performed by using the SYBR Green 1 detection method (Thermo Scientific). Cycle threshold (Ct) values were normalized to *Rn18s*, and the results were presented as fold over control. Primers for many of the genes investigated have been published (5), and additional primer sets used were as follows: *Acot7* (sense, 5′-TGACCAATAAAGCCACCTTGTG-3′; antisense, 5′-CCTGCTCCTGCCGTAAATACAC-3′); *Acot8* (sense, 5′-CCTCGAGCCGCTAGATGAAG-3′; antisense, 5′-GGCCCATAATTTGACCCCCA-3′); *Acot9* (sense, 5′-ACGGCTTTGGACCTTGAACA-3′; antisense, 5′-CTCCAGACTGTGGATACGCC-3′); *Acot1* (sense, 5′-CATCGAGCCCCCTTACTTCC-3′; antisense, 5′-TTCCCCAACCTCCAAACCATC-3′); *Acot2* (sense, 5′-GTTGTGCCAACAGGATTGGAA-3′; antisense, 5′-GCTCAGCGTCGCATTTGTC-3′); *Acot11* (sense, 5′-AGGGGCTTCGCCTCTATGTT-3′; antisense, 5′-TCCGGTATCCTTCACCCTCTG-3′); *Acot13* (sense, 5′-AGCAGCATGACCCAGAACCTA-3′; antisense, 5′-GGAGCGTGCCCAGTTTATTAGTA-3′); *Acsl4* (sense, 5′-CTGGAAAGCAAACTGAAGGC-3′; antisense, 5′-AGGGATACGTTCACACTGGC-3′); and *Tlr4* (sense, 5′-TTTGACACCCTCCATAGACTTCA-3′; antisense 5′-GAAACTGCAATCAAGAGTGCTG-3′).

IL-6, TNF-α, IL-1β, and CCL2 ELISA kits (eBioscience) and PGE_2 ELISA kits (Cayman Chemical) were used to quantify secreted cytokines or PGE_2 in vitro. For detection of ACOT7 protein, total cell lysates (10–20 μg) were loaded onto SDS-PAGE gels, separated, and transferred onto nitrocellulose membranes. Detection was accomplished by using a rabbit polyclonal ACOT7 antibody (1:1,000 dilution, Abcam, Cambridge, UK, catalog no. ab85151) and a mouse monoclonal β-actin antibody (1:10,000 dilution; Sigma-Aldrich).

Determination of thioesterase activity and acyl-CoA species

Thioesterase enzymatic activity was determined in lysates of BMDMs from mice with hematopoietic ACOT7 deficiency or BMDMs overexpressing ACOT7 (by transduction with an *Acot7* ecotropic retrovirus). Cells were allowed to differentiate in L-conditioned medium for 7 days before the experiment and then harvested in Western lysis buffer containing protease (Santa Cruz Biotechnology, Dallas, TX, catalog no. sc29130) and phosphatase inhibitors. Samples were frozen before the enzymatic assay at −80°C without degradation. For the assays, 12.5–25 μg of protein lysate and DTNB (Cayman Chemical) were incubated

with 150 nmol of various acyl-CoAs [Sigma-Aldrich (16:0-CoA, 18:1-CoA, 20:4-CoA) and Avanti Polar Lipids, Alabaster, AL (20:5-CoA 22:6-CoA)] in buffer containing: 50 mM KCl, 10 mM HEPES (pH 7.2), 0.025% Triton X-100, and 0.2 mg/ml FA-free BSA. The assays were performed under V_{max} conditions. Free CoA reacted with DTNB and was detected by measuring absorbance at 412 nm. Quantification was performed by using a standard curve of known CoA concentration (Sigma-Aldrich). In some experiments, ACOT7 was immunoprecipitated before the thioesterase activity assay. ACOT7 was immunoprecipitated by using a rabbit polyclonal anti-ACOT7 (ab8515; 1:1,000, Abcam). A nonspecific rabbit IgG was used for control immunoprecipitations. Briefly, cell lysates at a concentration of 1 mg of protein in 0.5 ml were incubated with 3 μg of ACOT7 antibody or IgG overnight. Target proteins bound by the antibodies were immunoprecipitated by the addition of protein G-agarose beads (Protein G-agarose Immunoprecipitation Kit, Roche Diagnostics, Basel, Switzerland) and incubation for 3 h. Antibody-conjugated beads were washed several times according to the manufacturer's protocol before the thioesterase assay. Each sample absorbance was normalized to its no substrate control before quantification of CoA released. All reactions were performed within the linear range. Measurements of acyl-CoA molecular species were performed by LC/ESI-MS/MS, as described previously (26).

Analysis of phospholipids by LC-MS/MS

WT and ACOT7-deficient BMDMs were stimulated with LPS (10 ng/ml) for 24 h. The cells were then quickly harvested in PBS and frozen at −80°C. Phospholipids were extracted from the cell pellets and analyzed by the Mass Spectrometry Lipidomics Core facility at the University of Colorado essentially as described (27), with some modifications. A commercial mixture of internal standards was used (SPLASH Lipidomix, from Avanti Polar Lipids, Inc.; 1 μl/sample) that contained 15:0/[$^2H_7$]18:1-PA (7 ng), 15:0/[$^2H_7$]18:1-PC (160 ng), 15:0/[$^2H_7$]18:1-PE (5 ng), 15:0/[$^2H_7$]18:1-PG (30 ng), 15:0/[$^2H_7$]18:1-PI (10 ng), and 15:0/[$^2H_7$]18:1-PS (5 ng). LC-MS/MS analysis was carried out in a system equipped with a HPLC system (Shimadzu, Kyoto, Japan) and a 4000 QTRAP mass spectrometer (SCIEX, Framingham, MA), using a scheduled multiple reaction monitoring (MRM) method to detect molecular species containing combinations of common fatty-acyl chains. The precursor ions monitored were molecular ions $[M-H]^-$ for all classes except PC, for which the acetate adducts $[M+CH3COO]^-$ were monitored. The product ions analyzed after collision-induced decomposition were carboxylate anions corresponding to one of the acyl chains. A scheduled MRM window width of 450 s was used, centered on the following elution times: PA, 24.3 min; PC, 29 min; PE, 17 min; PG and BMP, 8 min; PI, 15 min; and PS, 23 min. Supplemental Table S1 contains a complete list of the *m/z* transitions used. Results were analyzed by using MultiQuant software (SCIEX) and are reported as the ratio between the integrated area of each analyte and the integrated area of the corresponding internal standard for each class.

Generation of nondiabetic and diabetic mice lacking ACOT7 in bone marrow cells for atherosclerosis study

Bone marrow was harvested from ACOT7-deficient (ACOT7 KO) mice or WT controls (12), purified of erythrocytes, and transplanted into lethally irradiated (10 Gy) female $Ldlr^{-/-}$ recipients (5×10^6 cells injected retroorbitally). The mice were maintained on antibiotic (2 mg/ml neomycin) water for 2 weeks after the transplant and allowed to recover for a total of 7 weeks before streptozotocin (STZ) injections. STZ (mixed anomers no. S0130, 50 mg/kg; Sigma-Aldrich) was dissolved in freshly made citrate buffer (0.1 M, pH 4.5) and injected intraperitoneally for five consecutive days. The mice were monitored for development of diabetes (defined as blood glucose >250 mg/dl). If mice did not respond to the STZ treatment 14 days after the first injection, they were reinjected for an additional round of 5 days. In the present study, 37/40 mice exhibited blood glucose values >250 mg/dl. Blood glucose was monitored throughout the study by using test strips (One Touch Ultra, LifeScan, Milpitas, CA), and diabetic mice received insulin (Lantus, Sanofi-Aventis, Bridgewater, NJ) as needed to prevent excessive weight loss and ketonuria. After induction of diabetes, the mice were fed a semipurified low-fat diet for the duration of the 12-week study. This diet has been described previously (28) and is used because diabetic mice do not exhibit hypercholesterolemia as compared with nondiabetic controls when fed this diet. Blood cholesterol was measured by using test strips (Cardiochek, Indianapolis, IN). Plasma lipids were determined by colorimetric assays according to manufacturers' instructions: triglycerides (Sigma-Aldrich), NEFAs (Wako, Richmond, VA), and cholesterol (Wako). For mRNA measurements in leukocytes, mRNA was extracted from blood leukocytes according to manufacturer's instructions (Macherey Nagel; Nucleospin RNA kit). Aortas were dissected longitudinally and stained en face with Sudan IV for visualization of aortic lesions (28). Lesions were quantified in a blinded manner as percent area of the entire aortic area.

Statistical analysis

Statistical analyses for all studies were performed by using GraphPad Prism 5 software (GraphPad, La Jolla, CA). Unpaired two-tailed Student's *t*-test was used to compare two conditions, whereas multiple groups were compared by one-way ANOVA with a Tukey post hoc test or two-way ANOVA. Enzymatic activity assays were assessed by repeated-measures two-way ANOVA. For lipidomic data, volcano plots were generated to identify patterns of changes and followed up by one-way ANOVA for selected lipid species meeting nominal statistical significance and at least a 2-fold difference in the volcano plots. Error bars indicate SEM. $*P < 0.05$; $**P < 0.01$; $***P < 0.001$; $****P < 0.0001$.

RESULTS

ACOT7 is induced in macrophages through TLR4/MyD88 and is elevated in Ly6C^{high} monocytes as compared with Ly6C^{low} monocytes

Macrophages can become classically activated and promote inflammation or can become alternatively activated with wound-healing functions and antiinflammatory properties. The bacterial component LPS induces classical activation of macrophages, and ACOT7 has been previously shown to be induced in these cells by LPS (21). We first verified that in mouse thioglycollate-elicited macrophages and BMDMs *Acot7* mRNA and ACOT7 protein are increased after treatment with LPS (**Fig. 1A–**D). *Acot7* mRNA levels peaked at 6 h after stimulation and then declined (Fig. 1A). For comparison, *Acsl1* was more robustly induced by LPS (Fig. 1A). Furthermore, a significant increase in ACOT7 protein levels was observed up to 48 h after LPS stimulation (Fig. 1B). Similar results were obtained in BMDMs stimulated by LPS/IFNγ (data not shown). Moreover, ACOT7-specific CoA thioesterase activity, measured in ACOT7 immunoprecipitates, was increased by 3.1 ± 0.4-fold

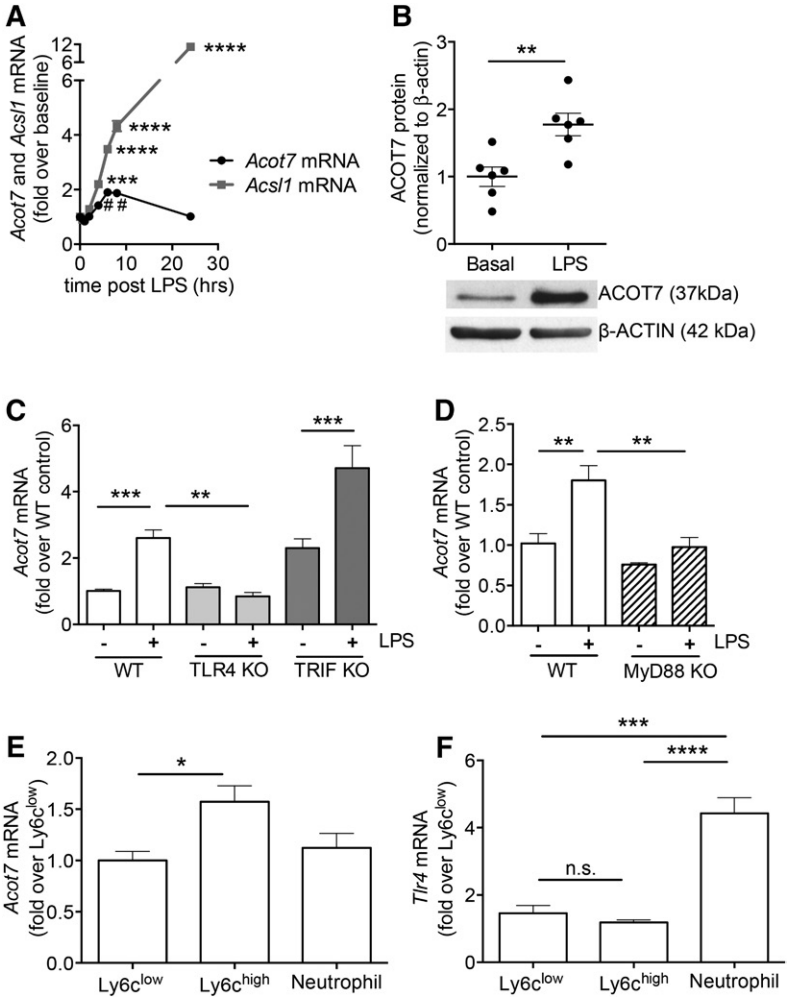

Fig. 1. ACOT7 is upregulated in response to LPS via the MyD88 arm of the TLR4 pathway. Thioglycollate-elicited macrophages exhibit increased *Acot7* and *Acsl1* mRNA (A) and ACOT7 protein (B) in response to LPS. BMDMs from *Tlr4*$^{-/-}$ (TLR4 KO), *Ticam1*$^{-/-}$ (TRIF KO) (C), and *Myd88*$^{-/-}$ (MyD88 KO) (D) mice were treated with 10 ng/ml ultrapure LPS for 4–6 h. *Acot7* mRNA expression is elevated in Ly6c^{high} blood monocytes (E), but did not coincide with *Tlr4* mRNA expression (F). *Acot7* mRNA was measured by real-time PCR, and ACOT7 protein was measured by Western blot analysis. Results are expressed as mean ± SEM (n = 3–6). Statistical analysis was performed by ANOVA (A, C–F) or two-tailed unpaired Student's *t*-test (B). * $P < 0.05$; ** $P < 0.01$; *** $P < 0.001$; **** $P < 0.0001$ versus t = 0 for *Acsl1* mRNA (A) or versus indicated group; $^{\#\#}P < 0.01$ versus t = 0 for *Acot7* mRNA (A). n.s., not significant.

in BMDMs stimulated with LPS/IFNγ as compared with IL-4 for 48 h ($P = 0.01$; n = 4), reflective of the increase in ACOT7 protein after LPS/IFNγ polarization. Thus, ACOT7 mRNA and protein are increased after LPS stimulation in macrophages, leading to greater ACOT7-specific thioesterase activity in these cells.

LPS is a ligand of TLR4, which, when activated, signals through two adaptor proteins: Toll/Il-1 receptor domain containing adaptor inducing IFN-β (TRIF; gene name *Ticam1*) and MyD88. We investigated the adaptor protein responsible for LPS-induced *Acot7* by taking advantage of BMDMs from *Tlr4*$^{-/-}$ and *Ticam1*$^{-/-}$ mice (Fig. 1C). BMDMs isolated from *Tlr4*$^{-/-}$ mice exhibited no increase in *Acot7* mRNA levels after LPS stimulation, as expected, whereas BMDMs from *Ticam1*$^{-/-}$ mice had normal, or even elevated, induction of *Acot7* mRNA after LPS stimulation. Therefore, regulation of ACOT7 after LPS treatment in macrophages is entirely dependent on TLR4 signaling, but does not require the TRIF adaptor protein. In an additional experiment using BMDMs from *Myd88*$^{-/-}$ mice, we demonstrated that induction of *Acot7* mRNA requires MyD88 (Fig. 1D).

Ly6C^{high} monocytes acutely traffic to regions of inflammation via CCR2 signaling and differentiate into macrophages (29). Flow cytometry was used to sort blood leukocytes into Ly6C^{high} monocytes, Ly6C^{low} monocytes, and neutrophils, and *Acot7* mRNA levels were determined in each of these populations. *Acot7* mRNA was elevated in the Ly6C^{high} monocyte population, as compared with the Ly6C^{low} monocyte population, suggesting a greater role for the enzyme in the Ly6C^{high} population (Fig. 1E). Because *Acot7* mRNA expression is downstream of TLR4 activation, *Tlr4* mRNA was assessed as well (Fig. 1F). *Tlr4* mRNA levels did not follow the same expression pattern as *Acot7* mRNA, suggesting that ACOT7 regulation in myeloid cell populations may be influenced by multiple factors in vivo.

Loss of ACOT7 reduces cellular 20:4-CoA, 20:5-CoA, and 22:6-CoA thioesterase activity

Previous studies on recombinant mouse ACOT7 demonstrated that ACOT7 prefers 20:4-CoA over saturated acyl-CoAs of various chain lengths (21). In order to confirm and expand these observations, first, we investigated whether loss of ACOT7 in macrophages is sufficient to lead to an overall reduction in 20:4-CoA hydrolysis. Loss of ACOT7 was achieved by harvesting bone marrow from whole-body *Acot7*$^{-/-}$ mice and differentiating these cells into BMDMs or by transfecting thioglycollate-elicited mouse peritoneal macrophages with *Acot7* siRNA (**Fig. 2A**–D). Both the BMDMs from *Acot7*$^{-/-}$ mice and peritoneal macrophages treated with *Acot7* siRNA exhibited a marked reduction in *Acot7* mRNA (Fig. 2A, B). ACOT7 protein was also markedly

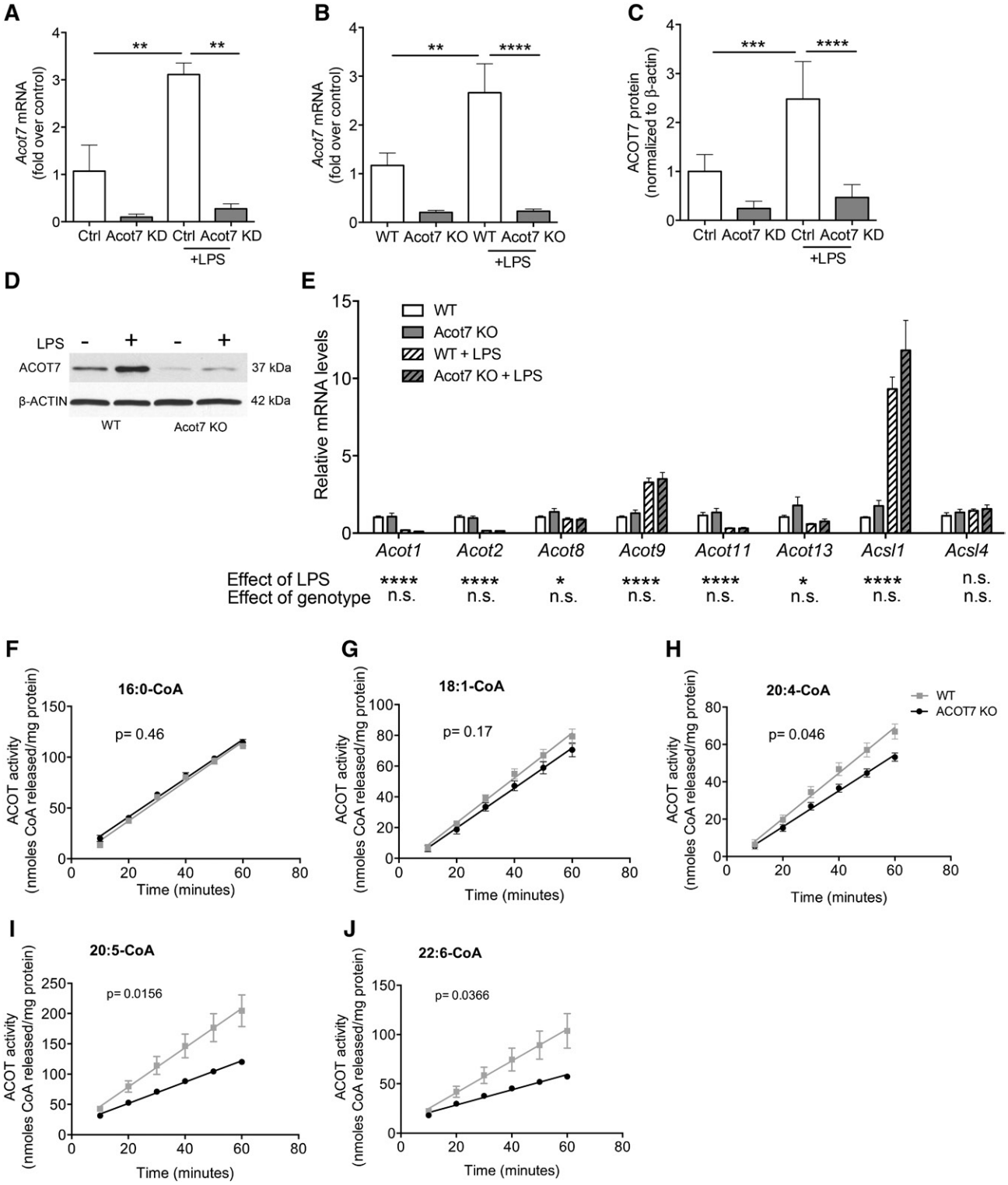

Fig. 2. ACOT7 KO and knockdown in macrophages results in reduced ACOT activity toward 20:4-CoA, 20:5-CoA, and 22:6-CoA. *Acot7* mRNA (A) and ACOT7 protein (C) were markedly knocked down in thioglycollate-elicited macrophages transfected with *Acot7* siRNA as compared with macrophages transfected with a control siRNA. BMDMs from ACOT7-deficient mice also were depleted of *Acot7* mRNA (B) and ACOT7 protein (D). BMDMs from *Acot7*$^{-/-}$ mice did not exhibit compensatory changes in *Acot1*, *Acot2*, *Acot8*, *Acot9*, *Acot11*, *Acot13*, *Acsl1*, or *Acsl4* 4 h after LPS stimulation (E). Thioesterase activity toward 16:0-CoA, 18:1-CoA, 20:4-CoA, 20:5-CoA, and 22:6-CoA was measured in BMDM cell lysates (F–J). Results are expressed as mean ± SEM (n = 7–8). Statistical analysis was performed by linear regression (F–J) or ANOVA. ** $P < 0.01$; *** $P < 0.001$; **** $P < 0.0001$. n.s., not significant.

reduced in both cell populations (Fig. 2C, D). There was no compensatory upregulation of other ACOTs expressed in macrophages, including *Acot1*, *Acot2*, *Acot8*, *Acot9*, *Acot11*, or *Acot13* (Fig. 2E). Furthermore, there was no compensatory regulation of *Acsl1* or *Acsl4* in ACOT7-deficient macrophages (Fig. 2E). Although most ACOTs exhibited reduced

mRNA expression after a 4 h LPS stimulation, *Acot9*, like *Acot7*, was significantly induced by LPS (Fig. 2E).

ACOT7-deficient macrophages did exhibit significantly less activity toward 20:4-CoA (1.22 ± 0.08 versus 0.96 ± 0.05 nmol/mg/min) as compared with WT controls, whereas activity toward 16:0-CoA and 18:1-CoA was similar to WT cells (1.95 ± 0.07 versus 1.90 ± 0.07 nmol/mg/min and 1.46 ± 0.07 versus 1.30 ± 0.08 nmol/mg/min, respectively) (Fig. 2F–H). These results suggest that endogenous ACOT7 in macrophages contributes significantly to total 20:4-CoA thioesterase activity, but that ACOT7 is not required for 18:1-CoA or 16:0-CoA thioesterase activity. We next tested ACOT activity toward the more unsaturated acyl-CoAs: 20:5-CoA and 22:6-CoA (Fig. 2I, J). Decreased activity toward 20:5-CoA and 22:6-CoA with loss of ACOT7 was even more pronounced than that toward 20:4-CoA (3.24 ± 0.41 versus 1.76 ± 0.07 nmol/mg/min and 1.61 ± 0.26 versus 0.77 ± 0.04 nmol/mg/min, respectively), suggesting that endogenous ACOT7 markedly contributes to 20:5-CoA and 22:6-CoA thioesterase activity.

In a separate set of experiments, ACOT7 was overexpressed 20- to 50-fold in J774 macrophages or BMDMs without compensation by other type II ACOTs selected for analysis (supplemental Fig. S1A–E). This led to an 11-fold increase in hydrolysis of 20:4-CoA (0.95 ± 0.06 versus 10.85 ± 0.61 nmol/mg/min), as compared with a 5-fold increase in 16:0-CoA hydrolysis and 6-fold increase in 18:1-CoA hydrolysis (1.71 ± 0.06 versus 9.09 ± 0.39 nmol/mg/min and 1.35 ± 0.06 versus 8.49 ± 0.27 nmol/mg/min, respectively) (supplemental Fig. S1F–H). ACOT7 overexpression also had very high activity toward the long-chain acyl-CoA species 20:5-CoA and 22:6-CoA (2.20 ± 0.03 versus 33.61 ± 0.68 nmol/mg/min and 0.96 ± 0.05 versus 15.54 ± 0.42 nmol/mg/min, respectively) (supplemental Fig. S1I, J). Thus, when overexpressed at high levels, ACOT7 contributes to thioesterase activity, affecting a wide variety of acyl-CoAs. On the contrary, corresponding acyl-CoAs quantified by LC/ESI-MS/MS were not significantly altered by ACOT7 overexpression in J774 macrophages (supplemental Fig. S1K–M). These data demonstrate that endogenous ACOT7 is required for efficient hydrolysis of 20:4-CoA, 20:5-CoA, and 22:6-CoA, and, although ACOT7 can have activity toward 18:1-CoA and 16:0-CoA, is not required for hydrolysis of these fatty acyl-CoAs in macrophage cell lysates, suggesting that other endogenous ACOTs are sufficient for this activity. Data from ACOT7 overexpression suggest that increased thioesterase activity is not sufficient to change the overall levels of acyl-CoA species; thus, these acyl-CoA species are rapidly replenished.

LPS stimulation results in a marked shift in BMP composition in the resolution phase of the inflammatory response

To investigate the effects of LPS stimulation at a time point at which ACOT7 is induced, we performed a lipidomic analysis of phospholipid molecular species in BMDMs under basal conditions and after a 24 h stimulation with LPS. A large majority of phospholipids altered in response to LPS were identified as BMPs. Interestingly, there was a dramatic shift in acyl-chain composition of BMPs in response to LPS, such that BMPs containing saturated and monounsaturated C14-C18 acyl-chains were reduced, and BMPs containing long C20-C22 polyunsaturated acyl-chains were enriched by LPS (**Fig. 3A**, D–H).

ACOT7 deficiency has a marginal effect on glycerophospholipids containing 20 carbon unsaturated acyl-chains

TLR4 activation profoundly remodels the lipidome in macrophages (6, 30), consistent with the results of the present study. Our lipidomic screen was conducted to assess changes in phospholipid species in macrophages with ACOT7 deficiency. Whereas LPS caused marked alterations in both WT and ACOT7-deficient macrophages, primarily in BMPs (Fig. 3A, B), ACOT7 deficiency did not have a striking

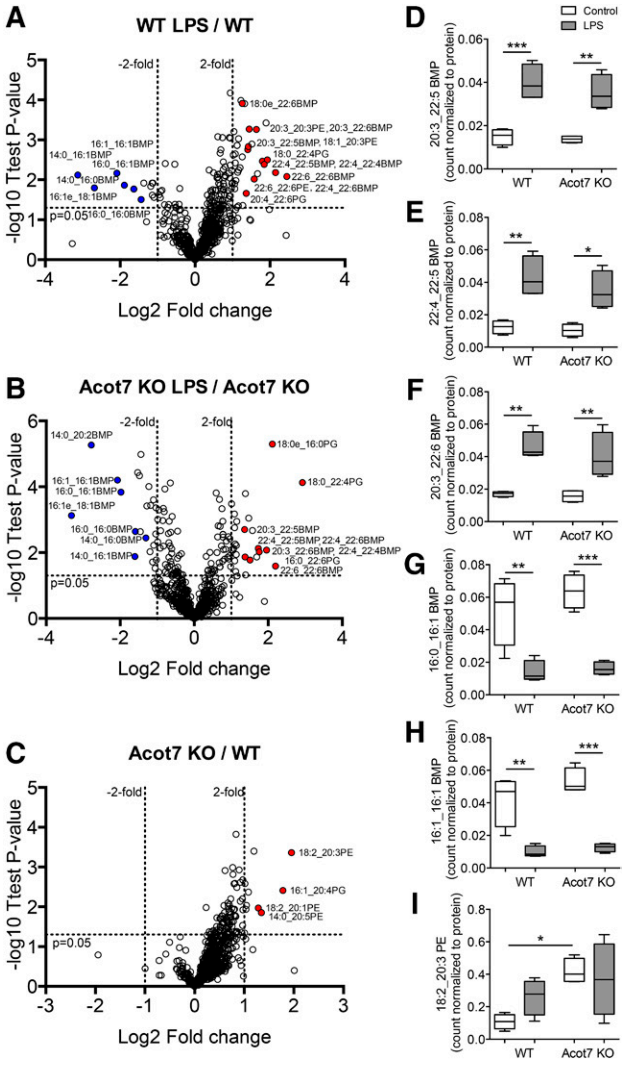

Fig. 3. LPS stimulation results in a marked shift in BMP acyl-chain length and saturation, whereas ACOT7 deficiency has a marginal effect. A lipidomic screen was used to assess alterations in 686 identified glycerophospholipids. LPS resulted in significant changes in BMDMs 24 h after stimulation (A, B, D–H), but few changes resulting from ACOT7 deficiency (C, I). Select species are identified in volcano plots comparing conditions (A–C), and selected species were further analyzed by one-way ANOVA (D–I). Statistical analysis was performed by ANOVA. * $P < 0.05$; ** $P < 0.01$; *** $P < 0.001$; **** $P < 0.0001$.

overall effect on BMPs or other phospholipids (Fig. 3C and supplemental Tables S2–S6). Interestingly, ACOT7 deficiency did not significantly alter arachidonic acid-containing phospholipid species, despite its known action on 20:4-CoA (21). Less than a handful of phospholipids were increased by ACOT7 deficiency under basal conditions (Fig. 3C), and no effect of ACOT7 deficiency was detected in LPS-stimulated cells (supplemental Tables S2–S6). The few phospholipids nominally increased by ACOT7 deficiency all contained unsaturated 20-carbon acyl-chains (Fig. 3C, I).

Loss of ACOT7 does not reduce LPS-induced cytokine production, nor does ACOT7 expression influence PGE_2 secretion

We next investigated whether ACOT7 could modulate the overall inflammatory status of macrophages stimulated with LPS. BMDMs from ACOT7-deficient macrophages had similar levels of LPS-induced *Tnfa*, *Il6*, or *Ccl2* mRNA at both 4 h (**Fig. 4A**–C) and 24 h (Fig. 4D–F) after stimulation. Secretion of IL-6 or TNF-α, as measured 18–24 h after LPS stimulation, was also unchanged by loss of ACOT7 (Fig. 4G, H). PGE_2 release was measured to assess the effect of ACOT7 loss on eicosanoid mediators of inflammation. Surprisingly, based on previous results on forced expression of active ACOT7 (21), and despite the substrate preference of ACOT7 for 20:4-CoA, PGE_2 release was unchanged by ACOT7 deficiency (Fig. 4I).

We also investigated cytokine expression in LPS-stimulated J774 macrophages overexpressing ACOT7 at high levels. Overexpression of ACOT7 resulted in increased secretion of IL-1β, TNF-α, and IL-6 after LPS stimulation (supplemental Fig. S2A–C). The mechanism for this increase in inflammation is unknown, but likely does not involve eicosanoid signaling because PGE_2 was not affected by ACOT7 overexpression, either under basal conditions or after LPS stimulation (supplemental Fig. S2D), nor was the effect ACOT7 on LPS-stimulated IL-6 release blocked by cyclooxygenase 2 and 5-lipoxygenase inhibitors (CAY 10404 and CJ-13,610, respectively) (supplemental Fig. S2E). It is likely that high levels of forced ACOT7

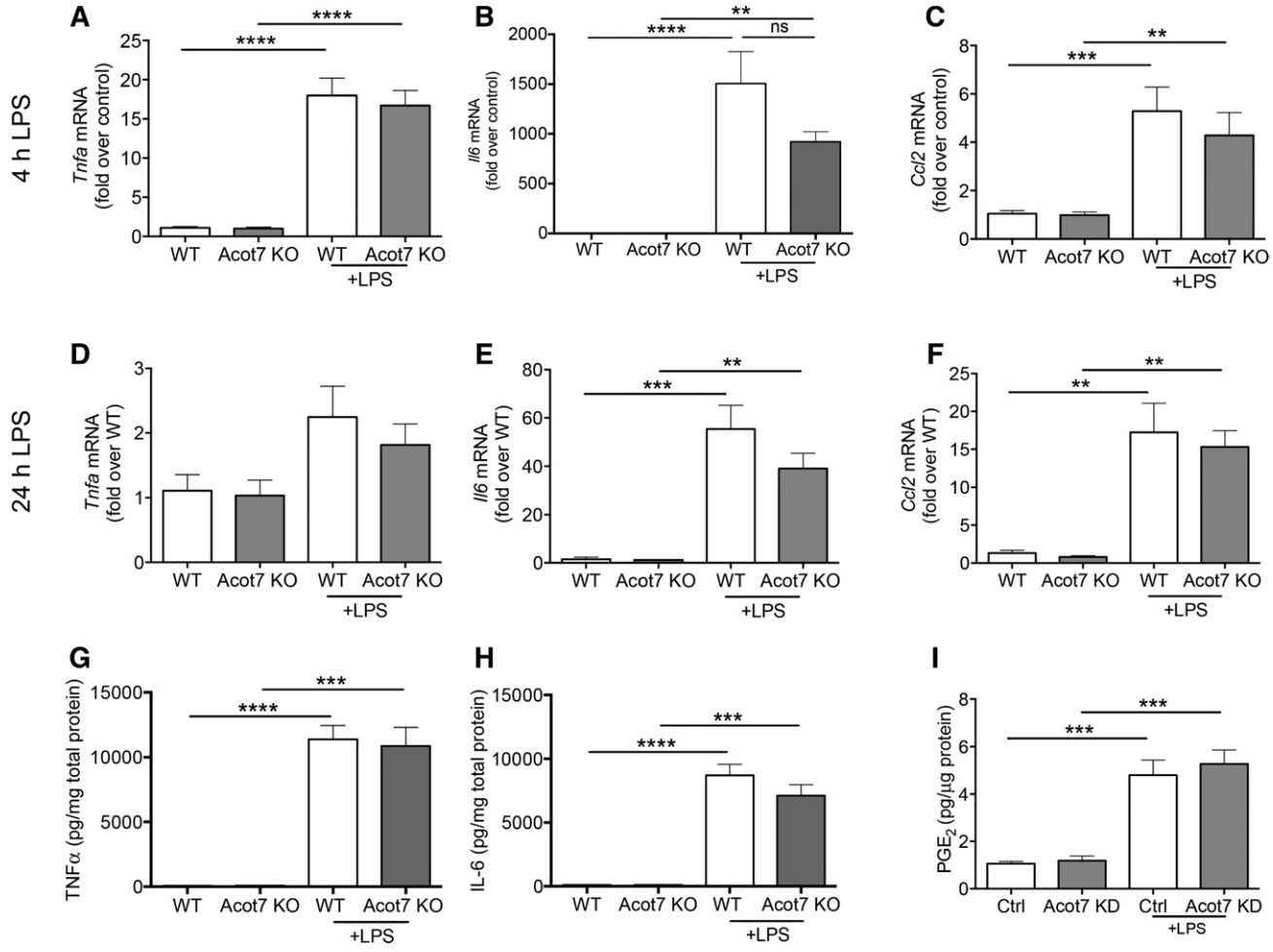

Fig. 4. ACOT7 deficiency does not affect LPS-induced inflammatory activation. ACOT7-deficient BMDMs were used to evaluate the role of ACOT7 on cytokine production, whereas PGE_2 secretion was analyzed in BMDMs in which ACOT7 had been knocked down by siRNA (and BMDMs treated with an siRNA control). The BMDMs were stimulated with 10 ng/ml LPS for 4 or 24 h or left unstimulated. *Tnfa* (A, D), *Il6* (B, E) ,and *Ccl2* (C, F) mRNA levels were measured by real-time PCR. Secretion of TNF-α (G), IL-6 (H), and PGE_2 (I) was measured by ELISA 18–24 h after LPS stimulation. Results are expressed as mean ± SEM (n = 3–6). Statistical analysis was performed by ANOVA. ** $P < 0.01$; *** $P < 0.001$; **** $P < 0.0001$. ns, not significant.

overexpression results in cellular changes in lipid pools that do not reflect physiological conditions, which is supported by our ACOT activity assay results.

Alternative activation of ACOT7-deficient BMDMs was assessed after 24 h of IL-4 treatment and compared with that of classical activation with low dose (0.1 ng/ml) LPS. Low-dose LPS elicited an increase in *Acot7* mRNA (supplemental Fig. S3A). IL-4 treatment increased expression of markers of alternative activation, but did not alter *Acot7* mRNA, nor did ACOT7 deficiency influence the response to IL-4 (supplemental Fig. S3A–D).

ACOT7 is modestly increased in macrophages from diabetic mice, but hematopoietic ACOT7 deficiency does not prevent inflammation or early atherosclerosis in diabetic mice

TLR4 stimulation is thought to contribute to the proinflammatory phenotype of macrophages in diabetes (31, 32). We therefore investigated whether ACOT7 is upregulated in macrophages in a mouse model of diabetes and whether ACOT7 could modulate inflammation and atherosclerosis in vivo. Thioglycollate-elicited macrophages from diabetic mice expressed modestly more *Acot7* mRNA and ACOT7 protein than did their nondiabetic littermates (**Fig. 5A**, B). To test the effect of ACOT7 deficiency in bone marrow-derived cells in diabetic mice, bone marrow from $Acot7^{-/-}$ mice or age-matched WT control mice was transplanted into irradiated $Ldlr^{-/-}$ recipient mice. After recovery, a subset of mice received STZ to induce diabetes, and the mice were then fed a semipurified low fat diet for the duration of the 12 week study (Fig. 5C). A complete KO of macrophage ACOT7 protein was achieved and sustained for the duration of the experiment in mice transplanted with bone marrow from $Acot7^{-/-}$ mice (Fig. 5C). Diabetic mice exhibited increased plasma triglyceride levels, increased blood glucose, and decreased body weight, but had no changes in plasma NEFAs or cholesterol. Importantly, hematopoietic ACOT7 deficiency did not alter any of these parameters (Fig. 5D–H). At the end of the study, leukocytes from mice transplanted with $Acot7^{-/-}$ bone marrow maintained significant knockdown of *Acot7* mRNA, as compared with those transplanted with WT bone marrow (Fig. 5I). Levels of *Il1b* mRNA in blood leukocytes were used to evaluate low-grade inflammation associated with diabetes. *Il1b* was elevated in leukocytes in mice with diabetes, but loss of hematopoietic ACOT7 did not alter this marker of inflammation in diabetic mice (Fig. 5J). Another ACOT induced by LPS in macrophages, *Acot9*, was not significantly affected by ACOT7 deficiency or diabetes (Fig. 5K). Although diabetes has been noted to increase TLR4 expression in monocytes (31–33) and ACOT7 expression in macrophages, presence of diabetes did not result in upregulation of *Acot7* or *Tlr4* mRNA in whole-blood leukocyte preparations in this study (Fig. 5I, L). Most mice developed early macrophage-rich atherosclerotic lesions after 12 weeks of diabetes, but hematopoietic ACOT7 deficiency did not alter the effect of diabetes on atherosclerosis (Fig. 5M). Nondiabetic mice had no lesions or very small lesions at this time point (Fig. 5M).

Together, these results suggest that subtle increases in ACOT7 expression, such as those seen in macrophages from diabetic mice, do not mediate macrophage accumulation in the artery wall or inflammation associated with diabetes. Failure of ACOT7 deficiency to alleviate the inflammatory response in LPS-stimulated macrophages supports this finding.

DISCUSSION

Modulation of the immune response by lipids and enzymes that control their metabolism and subcellular localization within the cell is an area of research that has attracted significant attention in recent years. There are now several examples of proteins involved in intracellular FA handling that are induced by inflammatory stimuli in macrophages (1, 3–6, 25). Our study is the first to investigate the effect of ACOT7 deficiency in macrophages. The results demonstrate that loss of ACOT7 in mouse macrophages is sufficient to reduce overall thioesterase activity toward 20:4-CoA, 20:5-CoA, and 22:6-CoA without significantly reducing thioesterase activity toward 16:0-CoA or 18:1-CoA, and that ACOT7 overexpression greatly increases thioesterase activity toward 20:4-CoA, 20:5-CoA, and 22:6-CoA and has a less dramatic effect on 16:0-CoA and 18:1-CoA. This validates previous work demonstrating that ACOT7 acts on 20:4-CoA in macrophages and adds omega-3 acyl-CoA species $\geq$20 carbons in length as important substrates for endogenous ACOT7. The preference of ACOT7 for 20:4-CoA over saturated acyl-CoA (C4:0 to C20:0) is consistent with the study of Forwood et al. (21) on recombinant mouse ACOT7. Our study furthers the findings by Forwood et al. (21) to include 20:5-CoA and 22:6-CoA, for which ACOT7 activity had not yet been examined. Furthermore, activity toward acyl-CoA substrates was assessed in whole-cell lysates; thus, although some thioesterase activity toward substrates $\geq$C20 remained, other enzymes with ACOT activity were not able to compensate for loss of ACOT7. Conversely, although ACOT7 can act on 16:0-CoA and 18:1-CoA in our overexpression model, endogenous ACOT7 is not required for complete cellular thioesterase activity toward these shorter acyl-CoA species in macrophage lysates. Our expanded cellular thioesterase activity assays suggest that a broader range of substrates for ACOT7 exists, which likely includes more unsaturated acyl-CoAs >20 carbons in length. Although it is possible that the effects of ACOT7 deficiency on some lipids are compensated for by other enzymes, it is also possible that ACOT7 may have a greater regulatory role of thioesterase activity in specific acyl-CoA pools or membrane compartments in vivo, which could explain the modest changes by ACOT7 deficiency on phospholipids containing 20-carbon unsaturated acyl-chains in the lipidomic data set. ACOT7 has been found to exhibit primarily a cytoplasmic localization in macrophages (7) (S.B., V.Z.W., and K.E.B., unpublished observations) and in other tissues (19, 34).

Forced expression of an active ACOT7 mutant in a macrophage cell line has been shown previously to reduce basal levels of PGD_2 and PGE_2 (21). Perturbations that affect FA

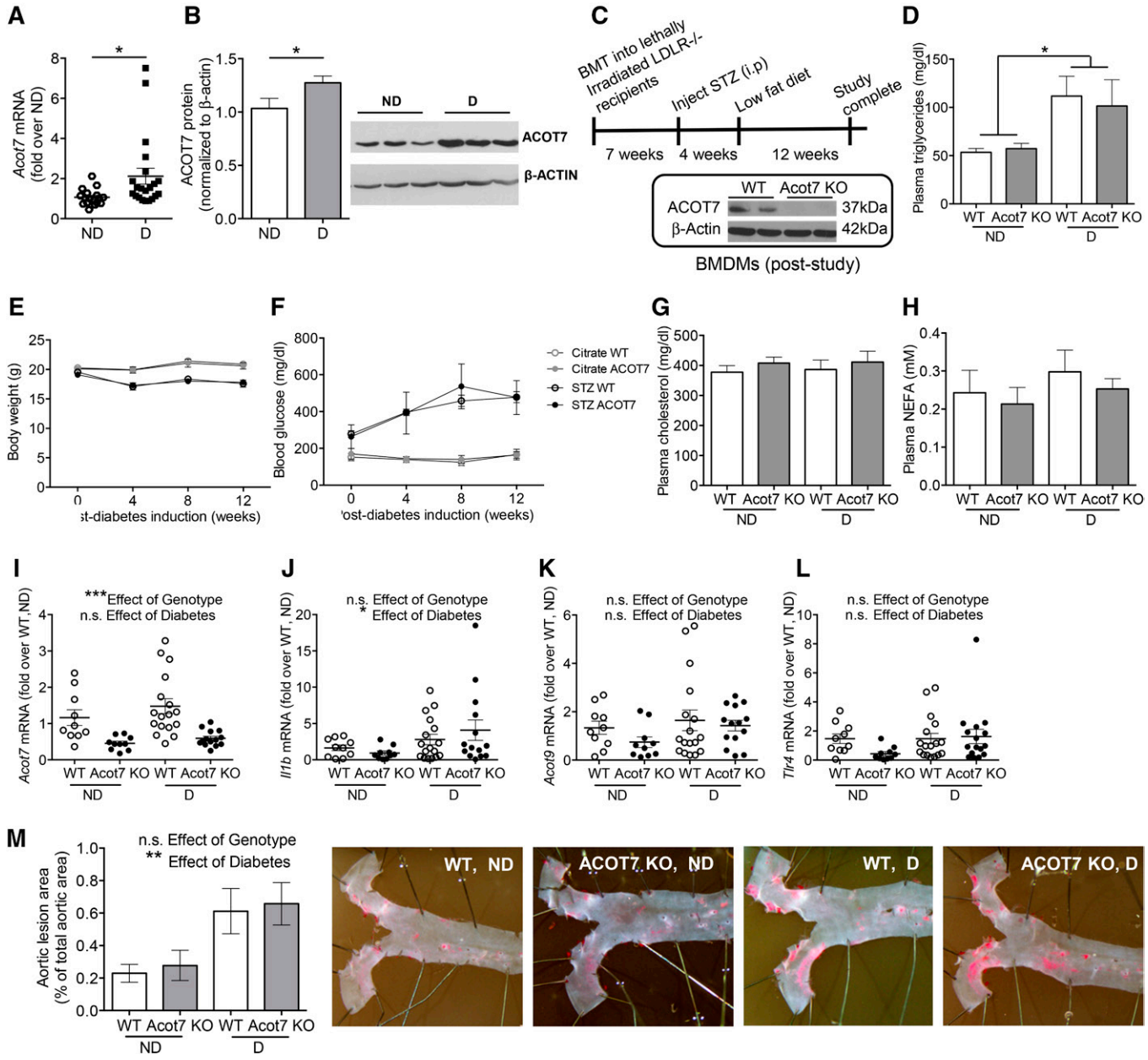

Fig. 5. Loss of ACOT7 in bone marrow-derived cells is not sufficient to prevent inflammation or atherosclerosis stimulated by diabetes. *Acot7* mRNA (A) and ACOT7 protein (B) were measured in thioglycollate-elicited macrophages from diabetic and nondiabetic *Ldlr*$^{-/-}$ mice by real-time PCR and Western blot analysis, respectively. Lethally irradiated female *Ldlr*$^{-/-}$ mice received bone marrow transplants (BMT) from *Acot7*$^{-/-}$ mice or WT controls, were allowed to recover for 7 weeks, and were then injected with STZ to induce diabetes. Some mice were injected with citrate and were used as nondiabetic controls. All mice were then fed a low-fat semipurified diet for 12 weeks (C). Isolated BMDMs harvested at the end of the study from mice that received *Acot7*$^{-/-}$ bone marrow had no detectable ACOT7 protein, showing a near complete chimerism (C). The bands shown are from the same blot and exposure times. Plasma triglycerides were measured at the end of the study (D). Body weights (E) and blood glucose (F) were measured every 4 weeks. Plasma cholesterol and NEFA were measured at the end of the study (G, H). At the end of the study, blood leukocytes were used for real-time PCR measurements of *Acot7* (I), *Il1b* (J), *Acot9* (K), and *Tlr4* (L). Atherosclerosis was evaluated by Sudan IV staining of the aorta using en face preparations and is expressed as percent lesion area of total aortic area (M). Representative en face preparations of the aortic arch are shown. Results are expressed as mean ± SEM (n = 10 nondiabetic; n = 15–17 diabetic). Statistical analysis was performed by Student's *t*-test (A, B) or two-way ANOVA. * $P < 0.05$; ** $P < 0.01$; *** $P < 0.001$. D, diabetic mice; ND, nondiabetic mice. n.s., not significant.

incorporation into phospholipids can have a profound effect on increasing eicosanoid synthesis (35). It has been hypothesized that the balance of 20:4-CoA/free 20:4 can be influenced by long-chain acyl-CoA hydrolases (36), such as ACOT7. However, our results clearly demonstrate that a large increase in overall 20:4-CoA thioesterase activity in macrophages overexpressing ACOT7 is not sufficient to reduce the steady-state pool of 20:4-CoA, suggesting that 20:4-CoA turnover is rapid, consistent with studies on other ACOTs. Accordingly, neither ACOT7 overexpression nor knockdown affected the ability of macrophages to produce PGE_2. These findings mimic other work in neurons lacking

ACOT7. In this tissue, a near complete loss of thioesterase activity did not alter levels of acyl-CoAs, PGE_2, or PGD_2 (12). Furthermore, the lipidomics suggests that ACOT7 deletion does not influence levels of 20:4-containing lipid species in basal conditions or their reorganization after LPS stimulation. This is highly suggestive of compensation by other enzymes in maintaining composition of 20:4-containing glycerophospholipids, even in the presence of significant reorganization. Because ACOT7 deficiency reduced thioesterase activity toward exogenously added 20:4-CoA in whole-cell lysates, it suggests that preservation of whole-cell glycerophospholipids containing 20:4 is accomplished by compensatory mechanisms beyond a simple rescue of thioesterase activity toward 20:4-CoA. However, it is possible that ACOT7 activity on 20:4-CoA is biologically relevant, but is limited to a distinct cellular pool that was not detectable in our whole-cell lipidome. Importantly, ACOT7 deficiency caused a greater reduction in activity toward 20:5-CoA and 22:6-CoA, suggesting that endogenous ACOT7 is a major thioesterase for these omega-3 acyl-CoAs in macrophages.

In neurons, where ACOT7 levels are high, expression of ACOT7 is positively regulated by binding of the transcription factor SREBP2 to the sterol regulatory element (SRE2) of the *Acot7* promoter region (37). In macrophages, SREBP1 has recently been shown to be responsible for inducing enzymes involved in MUFA and PUFA synthesis, which, in turn, drives the resolution phase of the inflammatory response to TLR4 activation in these cells (6). However, after LPS stimulation, *Acot7* mRNA is induced in the early phase of the inflammatory response, and its expression is decreased to near basal levels by 24 h, suggesting that SREBP1 may not be a major contributor to LPS-mediated induction of *Acot7* mRNA, although ACOT7 protein levels are elevated up to 48 h after LPS stimulation. We determined that MyD88, and not TRIF, is the adaptor protein required for TLR4-mediated ACOT7 induction in these cells. MyD88 signaling activates the transcription factors AP-1 and NF-κB (38). Thus, *Acot7* mRNA transcription in response to LPS in macrophages is likely downstream of one or more of these transcription factors. Similarly, ACSL1 is induced by PPARs in insulin target tissues, but not in macrophages, in which ACSL1 is induced by LPS and other inflammatory mediators (25). This suggests that ACOT7 in macrophages is part of the group of FA handling enzymes involved in the inflammatory response.

The lipidomics demonstrated that LPS has a marked effect on acyl-chain composition of BMPs, a phospholipid present in late endosomes (23, 39, 40), in macrophages. BMP (also known as lysobisphosphatidic acid) has been shown to be involved in transport of proteins and lipids, such as cholesterol, through the late endosome (41), and 22:6/22:6-BMP has been suggested to protect cholesterol from oxidation (42). Although our finding that LPS regulates BMP acyl-chain composition in macrophages will require further study, the data suggest that LPS modulates endosomal trafficking as part of the inflammatory and resolution response in macrophages. The finding that ACOT7 deficiency did not alter the acyl-chain composition of these BMPs in LPS-stimulated cells, although these BMPs are enriched in omega-3 and omega-6 acyl-chains, suggests that the role of ACOT7 is not to alter this aspect of cellular trafficking.

TLR4 is upregulated in monocytes from humans with type 1 diabetes (31, 33) and in a mouse model of the disease (32). Given that ACOT7 is induced by TLR4 activation, we hypothesized that expression of ACOT7 in macrophages would be altered in an STZ mouse model of diabetes and that it might influence the increased inflammatory response and atherosclerosis observed in diabetic mice. ACOT7 was indeed upregulated in macrophages from diabetic mice, although the extent of increase was modest. The increase in ACOT7 expression in the diabetic state may be specific to macrophages or myeloid cells, because diabetes did not significantly increase ACOT7 expression in the whole-blood leukocyte population. Hematopoietic ACOT7 deficiency did not inhibit diabetes-accelerated formation of early macrophage-rich lesions of atherosclerosis. Thus, although forced overexpression of ACOT7 at high levels has proinflammatory effects after LPS stimulation, it does not explain the increased inflammation and atherosclerosis associated with diabetes. Although our work describes the mechanism of *Acot7* mRNA induction in response to LPS, it is likely that *Acot7* transcription in macrophages is induced by additional stimuli in vivo and could use alternate signaling molecules downstream of these stimuli. Future studies will reveal whether ACOT7 plays a role in other immune cells and other inflammatory conditions, such as sepsis or various types of bacterial or viral infection.

In summary, ACOT7 is induced by TLR4-MyD88 activation and diabetes in macrophages. ACOT7 contributes a significant fraction of thioesterase activity toward C20:4-CoA, C20:5-CoA, and C22:6-CoA in macrophages, but is not required for LPS-induced reorganization of glycerophospholipids, particularly BMPs, containing unsaturated acyl-chains 20 carbon or longer. The functional outcome that ACOT7 may have on cellular processes in macrophages requires further investigation.

The authors thank Samuel T. Marionni and Nathan Basisty for consultation on analysis of mass spectrometry datasets.

REFERENCES

1. Makowski, L., K. C. Brittingham, J. M. Reynolds, J. Suttles, and G. S. Hotamisligil. 2005. The fatty acid-binding protein, aP2, coordinates macrophage cholesterol trafficking and inflammatory activity. Macrophage expression of aP2 impacts peroxisome proliferator-activated receptor gamma and IkappaB kinase activities. *J. Biol. Chem.* **280:** 12888–12895.
2. Furuhashi, M., G. Tuncman, C. Z. Gorgun, L. Makowski, G. Atsumi, E. Vaillancourt, K. Kono, V. R. Babaev, S. Fazio, M. F. Linton, et al. 2007. Treatment of diabetes and atherosclerosis by inhibiting fatty-acid-binding protein aP2. *Nature.* **447:** 959–965.
3. Babaev, V. R., R. P. Runner, D. Fan, L. Ding, Y. Zhang, H. Tao, E. Erbay, C. Z. Gorgun, S. Fazio, G. S. Hotamisligil, et al. 2011. Macrophage Mal1 deficiency suppresses atherosclerosis in low-density lipoprotein receptor-null mice by activating peroxisome proliferator-activated receptor-gamma-regulated genes. *Arterioscler. Thromb. Vasc. Biol.* **31:** 1283–1290.
4. Xu, H., A. V. Hertzel, K. A. Steen, Q. Wang, J. Suttles, and D. A. Bernlohr. 2015. Uncoupling lipid metabolism from inflammation

through fatty acid binding protein-dependent expression of UCP2. *Mol. Cell. Biol.* **35:** 1055–1065.
5. Kanter, J. E., F. Kramer, S. Barnhart, M. M. Averill, A. Vivekanandan-Giri, T. Vickery, L. O. Li, L. Becker, W. Yuan, A. Chait, et al. 2012. Diabetes promotes an inflammatory macrophage phenotype and atherosclerosis through acyl-CoA synthetase 1. *Proc. Natl. Acad. Sci. USA.* **109:** E715–E724.
6. Oishi, Y., N. J. Spann, V. M. Link, E. D. Muse, T. Strid, C. Edillor, M. J. Kolar, T. Matsuzaka, S. Hayakawa, J. Tao, et al. 2017. SREBP1 contributes to resolution of pro-inflammatory TLR4 signaling by reprogramming fatty acid metabolism. *Cell Metab.* **25:** 412–427.
7. Kirkby, B., N. Roman, B. Kobe, S. Kellie, and J. K. Forwood. 2010. Functional and structural properties of mammalian acyl-coenzyme A thioesterases. *Prog. Lipid Res.* **49:** 366–377.
8. Brocker, C., C. Carpenter, D. W. Nebert, and V. Vasiliou. 2010. Evolutionary divergence and functions of the human acyl-CoA thioesterase gene (ACOT) family. *Hum. Genomics.* **4:** 411–420.
9. Ellis, J. M., C. E. Bowman, and M. J. Wolfgang. 2015. Metabolic and tissue-specific regulation of acyl-CoA metabolism. *PLoS One.* **10:** e0116587.
10. Hunt, M. C., J. Yamada, L. J. Maltais, M. W. Wright, E. J. Podesta, and S. E. Alexson. 2005. A revised nomenclature for mammalian acyl-CoA thioesterases/hydrolases. *J. Lipid Res.* **46:** 2029–2032.
11. Zhuravleva, E., H. Gut, D. Hynx, D. Marcellin, C. K. Bleck, C. Genoud, P. Cron, J. J. Keusch, B. Dummler, M. D. Esposti, et al. 2012. Acyl coenzyme A thioesterase Them5/Acot15 is involved in cardiolipin remodeling and fatty liver development. *Mol. Cell. Biol.* **32:** 2685–2697.
12. Ellis, J. M., G. W. Wong, and M. J. Wolfgang. 2013. Acyl coenzyme A thioesterase 7 regulates neuronal fatty acid metabolism to prevent neurotoxicity. *Mol. Cell. Biol.* **33:** 1869–1882.
13. Moffat, C., L. Bhatia, T. Nguyen, P. Lynch, M. Wang, D. Wang, O. R. Ilkayeva, X. Han, M. D. Hirschey, S. M. Claypool, et al. 2014. Acyl-CoA thioesterase-2 facilitates mitochondrial fatty acid oxidation in the liver. *J. Lipid Res.* **55:** 2458–2470.
14. Kang, H. W., C. Ozdemir, Y. Kawano, K. B. LeClair, C. Vernochet, C. R. Kahn, S. J. Hagen, and D. E. Cohen. 2013. Thioesterase superfamily member 2/Acyl-CoA thioesterase 13 (Them2/Acot13) regulates adaptive thermogenesis in mice. *J. Biol. Chem.* **288:** 33376–33386.
15. Kang, H. W., M. W. Niepel, S. Han, Y. Kawano, and D. E. Cohen. 2012. Thioesterase superfamily member 2/acyl-CoA thioesterase 13 (Them2/Acot13) regulates hepatic lipid and glucose metabolism. *FASEB J.* **26:** 2209–2221.
16. Zhang, Y., Y. Li, M. W. Niepel, Y. Kawano, S. Han, S. Liu, A. Marsili, P. R. Larsen, C. H. Lee, and D. E. Cohen. 2012. Targeted deletion of thioesterase superfamily member 1 promotes energy expenditure and protects against obesity and insulin resistance. *Proc. Natl. Acad. Sci. USA.* **109:** 5417–5422.
17. Martinez-Sanchez, A., T. J. Pullen, P. Chabosseau, Q. Zhang, E. Haythorne, M. C. Cane, M. S. Nguyen-Tu, S. R. Sayers, and G. A. Rutter. 2016. Disallowance of Acot7 in beta-cells is required for normal glucose tolerance and insulin secretion. *Diabetes.* **65:** 1268–1282.
18. Okada, K., K. B. LeClair, Y. Zhang, Y. Li, C. Ozdemir, T. I. Krisko, S. J. Hagen, R. A. Betensky, A. S. Banks, and D. E. Cohen. 2016. Thioesterase superfamily member 1 suppresses cold thermogenesis by limiting the oxidation of lipid droplet-derived fatty acids in brown adipose tissue. *Mol. Metab.* **5:** 340–351.
19. Kuramochi, Y., M. Takagi-Sakuma, M. Kitahara, R. Emori, Y. Asaba, R. Sakaguchi, T. Watanabe, J. Kuroda, K. Hiratsuka, Y. Nagae, et al. 2002. Characterization of mouse homolog of brain acyl-CoA hydrolase: molecular cloning and neuronal localization. *Brain Res. Mol. Brain Res.* **98:** 81–92.
20. Yamada, J., A. Kurata, M. Hirata, T. Taniguchi, H. Takama, T. Furihata, K. Shiratori, N. Iida, M. Takagi-Sakuma, T. Watanabe, et al. 1999. Purification, molecular cloning, and genomic organization of human brain long-chain acyl-CoA hydrolase. *J. Biochem.* **126:** 1013–1019.
21. Forwood, J. K., A. S. Thakur, G. Guncar, M. Marfori, D. Mouradov, W. Meng, J. Robinson, T. Huber, S. Kellie, J. L. Martin, et al. 2007. Structural basis for recruitment of tandem hotdog domains in acyl-CoA thioesterase 7 and its role in inflammation. *Proc. Natl. Acad. Sci. USA.* **104:** 10382–10387.
22. Broustas, C. G., and A. K. Hajra. 1995. Purification, properties, and specificity of rat brain cytosolic fatty acyl coenzyme A hydrolase. *J. Neurochem.* **64:** 2345–2353.
23. Akgoc, Z., S. Iosim, and T. N. Seyfried. 2015. Bis(monoacylglycero) phosphate as a macrophage enriched phospholipid. *Lipids.* **50:** 907–912.
24. Schwenk, F., U. Baron, and K. Rajewsky. 1995. A cre-transgenic mouse strain for the ubiquitous deletion of loxP-flanked gene segments including deletion in germ cells. *Nucleic Acids Res.* **23:** 5080–5081.
25. Rubinow, K. B., V. Z. Wall, J. Nelson, D. Mar, K. Bomsztyk, B. Askari, M. A. Lai, K. D. Smith, M. S. Han, A. Vivekanandan-Giri, et al. 2013. Acyl-CoA synthetase 1 is induced by Gram-negative bacteria and lipopolysaccharide and is required for phospholipid turnover in stimulated macrophages. *J. Biol. Chem.* **288:** 9957–9970.
26. Nishizawa, T., J. E. Kanter, F. Kramer, S. Barnhart, X. Shen, A. Vivekanandan-Giri, V. Z. Wall, J. Kowitz, S. Devaraj, K. D. O'Brien, et al. 2014. Testing the role of myeloid cell glucose flux in inflammation and atherosclerosis. *Cell Rep.* **7:** 356–365.
27. Zarini, S., J. A. Hankin, R. C. Murphy, and M. A. Gijon. 2014. Lysophospholipid acyltransferases and eicosanoid biosynthesis in zebrafish myeloid cells. *Prostaglandins Other Lipid Mediat.* **113–115:** 52–61.
28. Renard, C. B., F. Kramer, F. Johansson, N. Lamharzi, L. R. Tannock, M. G. von Herrath, A. Chait, and K. E. Bornfeldt. 2004. Diabetes and diabetes-associated lipid abnormalities have distinct effects on initiation and progression of atherosclerotic lesions. *J. Clin. Invest.* **114:** 659–668.
29. Leuschner, F., P. Dutta, R. Gorbatov, T. I. Novobrantseva, J. S. Donahoe, G. Courties, K. M. Lee, J. I. Kim, J. F. Markmann, B. Marinelli, et al. 2011. Therapeutic siRNA silencing in inflammatory monocytes in mice. *Nat. Biotechnol.* **29:** 1005–1010.
30. Andreyev, A. Y., E. Fahy, Z. Guan, S. Kelly, X. Li, J. G. McDonald, S. Milne, D. Myers, H. Park, A. Ryan, et al. 2010. Subcellular organelle lipidomics in TLR-4-activated macrophages. *J. Lipid Res.* **51:** 2785–2797.
31. Devaraj, S., M. R. Dasu, J. Rockwood, W. Winter, S. C. Griffen, and I. Jialal. 2008. Increased toll-like receptor (TLR) 2 and TLR4 expression in monocytes from patients with type 1 diabetes: further evidence of a proinflammatory state. *J. Clin. Endocrinol. Metab.* **93:** 578–583.
32. Devaraj, S., P. Tobias, and I. Jialal. 2011. Knockout of toll-like receptor-4 attenuates the pro-inflammatory state of diabetes. *Cytokine.* **55:** 441–445.
33. Devaraj, S., I. Jialal, J. M. Yun, and A. Bremer. 2011. Demonstration of increased toll-like receptor 2 and toll-like receptor 4 expression in monocytes of type 1 diabetes mellitus patients with microvascular complications. *Metabolism.* **60:** 256–259.
34. Hunt, M. C., S. Greene, K. Hultenby, L. T. Svensson, S. Engberg, and S. E. Alexson. 2007. Alternative exon usage selectively determines both tissue distribution and subcellular localization of the acyl-CoA thioesterase 7 gene products. *Cell. Mol. Life Sci.* **64:** 1558–1570.
35. Goppelt-Struebe, M., C. F. Koerner, G. Hausmann, D. Gemsa, and K. Resch. 1986. Control of prostanoid synthesis: role of reincorporation of released precursor fatty acids. *Prostaglandins.* **32:** 373–385.
36. Sakuma, S., Y. Fujimoto, K. Doi, S. Nagamatsu, H. Nishida, and T. Fujita. 1994. Existence of an enzymatic pathway furnishing arachidonic acid for prostaglandin synthesis from arachidonoyl CoA in rabbit kidney medulla. *Biochem. Biophys. Res. Commun.* **202:** 1054–1059.
37. Takagi, M., F. Suto, T. Suga, and J. Yamada. 2005. Sterol regulatory element-binding protein-2 modulates human brain acyl-CoA hydrolase gene transcription. *Mol. Cell. Biochem.* **275:** 199–206.
38. Ostuni, R., I. Zanoni, and F. Granucci. 2010. Deciphering the complexity of Toll-like receptor signaling. *Cell. Mol. Life Sci.* **67:** 4109–4134.
39. Kobayashi, T., E. Stang, K. S. Fang, P. de Moerloose, R. G. Parton, and J. Gruenberg. 1998. A lipid associated with the antiphospholipid syndrome regulates endosome structure and function. *Nature.* **392:** 193–197.
40. Kobayashi, T., K. Startchev, A. J. Whitney, and J. Gruenber. 2001. Localization of lysobisphosphatidic acid-rich membrane domains in late endosomes. *Biol. Chem.* **382:** 483–485.
41. Kobayashi, T., M. H. Beuchat, M. Lindsay, S. Frias, R. D. Palmiter, H. Sakuraba, R. G. Parton, and J. Gruenberg. 1999. Late endosomal membranes rich in lysobisphosphatidic acid regulate cholesterol transport. *Nat. Cell Biol.* **1:** 113–118.
42. Bouvier, J., K. A. Zemski Berry, F. Hullin-Matsuda, A. Makino, S. Michaud, A. Geloen, R. C. Murphy, T. Kobayashi, M. Lagarde, and I. Delton-Vandenbroucke. 2009. Selective decrease of bis(monoacylglycero)phosphate content in macrophages by high supplementation with docosahexaenoic acid. *J. Lipid Res.* **50:** 243–255.